# Electronic Origin of Nonstoichiometry in Early-Transition-Metal Chalcogenides

Jeremy K. Burdett* and John F. Mitchell†

*Department of Chemistry and James Franck Institute, The University of Chicago, Chicago, Illinois 60637*

*Received April 19, 1993. Revised Manuscript Received July 21, 1993®*

Using cluster models and extended Hückel calculations on rocksalt supercells, we demonstrate that the transformation of square-planar S atoms to *cis*-divacant "butterflies" drives the ordering of Sc vacancies into alternating (111) metal planes in $Sc_{1-x}S$. Charge-iteration calculations show that metal vacancy formation arises from a combination of first-order shifts in the Sc d band with increasing nonstoichiometry and second-order mixing of the Sc 3d and S 3p bands. Such a mechanism explains why it is precisely for the early-transition-metal sulfides that this kind of nonstoichiometry is observed. Our extended Hückel results are corroborated by ideas from the method of moments and pair potential calculations.

## Introduction

The structure and properties of transition-metal sulfides has been an area of intense study for decades. As classical structure types, these compounds are frequently described in terms of close-packed arrays of sulfide ions with metal atoms occupying the octahedral interstices. Representatives of this building pattern are the layered 1:2 disulfides $TiS_2$ and $ZrS_2$, and the rocksalt-based 1:1 sulfides of groups 3 and 4. They have been extensively reviewed.[1,2] Despite the effort devoted to studying these materials, we still have much to learn about sulfide structures; the recent characterization of the fascinating "misfit" layer structures[3] underscores this point.

Of particular interest to us in this paper are the 1:1 binary sulfides of the group 3 and 4 transition metals, MS (M = Sc, Y, La, Ti, Zr, Hf), which have been of interest for some time because of the way vacancies form and order. Although there are many straightforward examples of solids with the rocksalt (NaCl), nickel arsenide (NiAs), and tungsten carbide (WC) structures, X-ray diffraction studies of these MS systems[4–9] have revealed that more complicated structures are often found in such binaries. In fact a surprising variety of ordered and disordered vacancy phases exist near the stoichiometric 1:1 composition, particularly among the rocksalt-based compounds. Indeed most, if not all, of these systems exhibit homogeneity ranges extending to either side of the 1:1 stoichiometry, with vacancies forming on either the metal sublattice, the sulfide sublattice, or both.[2,9] Often these vacancies at least partially order, as in the case of $Sc_{1-x}S$ and its relatives. In this system, the high-temperature phase has a random distribution of Sc vacancies on a fcc sublattice, the sulfide sublattice remaining unchanged.[10] Upon cooling, the vacancies order in alternating (111) metal planes, as shown in **1**. Although several thermodynamic

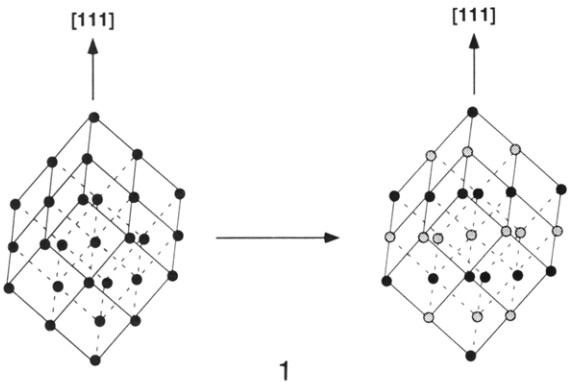


**1**

measurements and a few electronic structure calculations have been reported on the rocksalt phases, particularly by Franzen in the $Sc_{1-x}S$ series,[11–13] the driving force for such vacancy formation and ordering in these systems remains unclear. These are particularly interesting theoretically, as the long metal–metal separations indicate a minimal role for direct metal–metal bonding in the rocksalt phases, unlike their relatives in the NiAs structure.

Here we are interested in studying the order–disorder transition and vacancy formation in the rocksalt sulfide $Sc_{1-x}S$ from a purely theoretical standpoint. In a recent review we have argued that $Sc_{1-x}S$ is a structural prototype for the ordered defect structure of the 1:1 sulfides of many of these early transition metals.[14] It is important to note that nonstoichiometry on the metal sublattice is peculiar to early-transition-metal chalcogenides. Farther to the right in the periodic table, nonstoichiometric phases appear with anion deficiencies as well. Clearly, any reasonable

† Current address: Materials Science Division, Argonne National Laboratory, Argonne, IL 60439.

• Abstract published in *Advance ACS Abstracts,* September 1, 1993.

(1) Rao, C. N. R.; Pisharody, K. P. R. *Prog. Solid State Chem.* **1977,** *10,* 207.
(2) Wadsley, A. D. In *Non-Stoichiometric Compounds*; Mandelcorn, L., Ed.; Academic: New York, 1964; pp 98–209.
(3) Wiegers, G. A.; Meerschaut, A. *J. Alloys Compounds* **1992,** *178,* 351.
(4) Hahn, H.; Harder, B.; Mutschke, U.; Ness, P. *Z. Anorg. Allg. Chem.* **1957,** *292,* 82.
(5) Hahn, H.; Ness, P. *Z. Anorg. Allg. Chem.* **1959,** *302,* 17.
(6) Hahn, H.; Ness, P. *Z. Anorg. Allg. Chem.* **1959,** *302,* 37.
(7) Hahn, V. H.; Ness, P. *Z. Anorg. Allg. Chem.* **1959,** *302,* 136.
(8) McTaggart, F. K. *Aust. J. Chem.* **1958,** *11,* 471.
(9) McTaggart, F. K.; Wadsley, A. D. *Aust. J. Chem.* **1958,** *11,* 445.
(10) Dismukes, J. P.; White, J. G. *Inorg. Chem.* **1964,** *4,* 1220.
(11) Franzen, H. F.; Merrick, J. A. *J. Solid State Chem.* **1980,** *33,* 371.
(12) Franzen, H. F.; Nakahara, J. F.; Misemer, D. K. *J. Solid State Chem.* **1986,** *61,* 338.
(13) Misemer, D. K.; Nakahara, J. F. *J. Chem. Phys.* **1984,** *80,* 1964.
(14) Burdett, J. K.; Mitchell, J. M., manuscript in preparation.

0897-4756/93/2805-1465$04.00/0 

model of vacancy formation in the sulfides must account for this observation. Our goals then are 2-fold: to understand the ordering phenomenon in the (111) metal planes, and to determine why, upon heating ScS, Sc leaves the rocksalt lattice preferentially over S.

From the outset we note that these are challenging problems, as evidenced by the lack of theoretical work in this area. Indeed, we find only two theoretical papers in the recent literature concerned with this material.[12,13] Franzen and co-workers have performed calculations at the KKR level on small model systems, and we will comment later on these results as they relate to the present work. In this paper, after describing the electronic structure of the stoichiometric ScS phase, we proceed to look at the ordering problem from the standpoint of cluster models and extended systems, exploring the parallels between the two. On the basis of the notion that this and related materials may be microtwinned,[14] we also investigate the utility of our recently proposed order–disorder model[15] for microtwinned materials as it applies to the $Sc_{1-x}S$ system. We then turn to the question of the nonstoichiometry itself, namely, what is the electronic driving force behind it? Here we propose a model supported by extended Hückel tight-binding calculations that depends crucially on the fact that these systems are early-transition-metal systems with rather few electrons in the metal bands. Indeed, our model will specifically demonstrate that it is exactly under these conditions that loss of metal alone from the rocksalt structure is feasible.

## Electronic Structure of Stoichiometric ScS

ScS is a typical rocksalt sulfide. The size of the sulfide ion makes for a rather large lattice parameter (5.17 Å) and consequently a long Sc–Sc contact of 3.67 Å. With such a long metal–metal distance, we expect to see a clean separation of the metal-based energy bands into their $t_{2g}$ and $e_g$ components derived from the octahedron, the local symmetry about Sc. Further, because of the large separation between Sc atoms, we can expect little metal–metal bonding. (We note parenthetically that conductivity measurements unambiguously demonstrate that $Sc_{1-x}S$ is metallic.[10]) That is, the d electron is itinerant, and a band model is an appropriate description of the electronic structure. Within three well-resolved peaks, the extended Hückel DOS in Figure 1 bears out the first of our predictions (orbital parameters are tabulated in the appendix and are the result of charge iteration on ScS). Below −20 eV lies the S 3s band. While there is some admixture of Sc s and d character into this band, to all intents and purposes it is exclusively S located. Between roughly −16 and −12.5 eV lies the S 3p band. This band is also largely S, but has a significant component of Sc d; these are the Sc–S bonding orbitals. Finally, above −10 eV are the Sc d orbitals. Note the sharp peak at the bottom of this band. These are the $t_{2g}$ states, and the large Sc–Sc separation accounts for the narrow dispersion of these orbitals. The very bottom of the $t_{2g}$ band is strictly Sc–Sc bonding. From roughly −7.5 to −5 eV lie the $e_g$ bands, which contain significant S character. With formally one d electron, the Fermi level lies in the $t_{2g}$ region. Importantly, the conduction band orbitals at and below the Fermi energy are exclusively metal located. The bottom panel

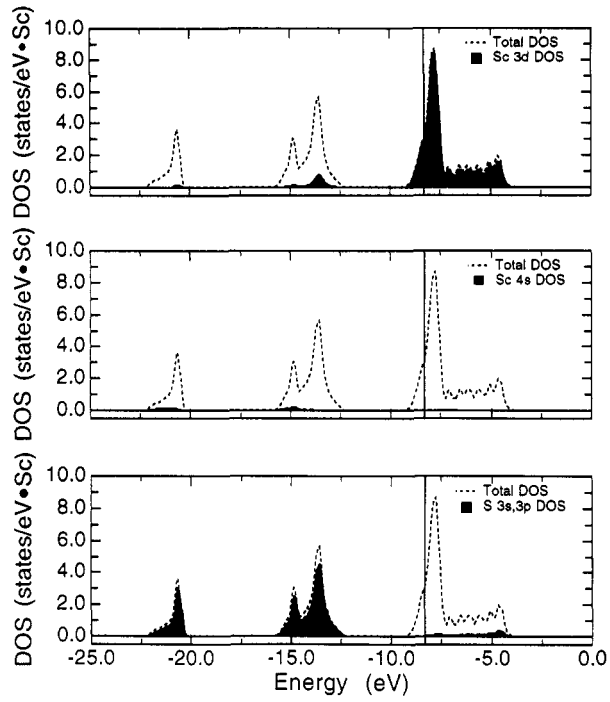


**Figure 1.** Density of states of stoichiometric ScS using charge-iterated parameters. Vertical line denotes the Fermi level for a $d^1$ transition metal.

of Figure 1 shows that the S component grows in above this energy. A powerful complement to the DOS is the crystal orbital overlap population (COOP) curve,[16–18] an overlap population-weighted DOS. Where it is positive, the states are bonding between the projected atoms; where it is negative, the states are antibonding. The COOP curves in Figure 2 show the Sc–Sc and Sc–S overlap populations and their integrals as a function of energy. Focusing first on the Sc–S COOP in the bottom panel, we see that indeed the bonding between Sc and S is maximized well below the Fermi level. Addition of electrons will weaken the bond, but oxidation of the metal via Sc loss should have little or no effect, at least in the rigid-band approximation. The Sc–Sc overlap opulation pictured in the top panel verifies our assumption of weak metal–metal bonding. Although the $d^1$ electron count seems to maximize the integrated COOP, it is quite small, a consequence of the long Sc–Sc contact. Thus on a rigid band model, oxidation of the metal leads to loss of electrons from orbitals which have no S character and are Sc–Sc bonding. There is no obvious mechanism for metal atom loss.

A similar viewpoint comes from a study of the Sc–Sc and S–S pair potentials. The idea of pair potentials is, of course, quite old, but we have recently explored their use in a wide range of systems, including organometallic complexes,[19] surfaces,[20–22] the 1-2-3 copper oxide superconductor,[23] and NbO and TiO.[24] The idea here is to see whether a repulsive pair interaction exists between atom

(15) Burdett, J. K.; Mitchell, J. M., submitted to *Phys. Rev B: Condens. Matter.*

(16) Hughbanks, T.; Hoffmann, R. *J. Am. Chem. Soc.* **1983**, *105*, 3528.
(17) Kertesz, M.; Hoffmann, R. *J. Am. Chem. Soc.* **1984**, *106*, 3453.
(18) Wijeyesekera, S. D.; Hoffmann, R. *Organometallics* **1984**, *3*, 949.
(19) Burdett, J. K.; Fässler, T. F. *Inorg. Chem.* **1991**, *30*, 2859.
(20) Burdett, J. K.; Czech, P. T.; Fässler, T. F. *Inorg. Chem.* **1992**, *31*, 129.
(21) Burdett, J. K.; Chung, J. T.; Pourian, M. R. *New J. Chem.* **1991**, *15*, 853.
(22) Burdett, J. K.; Fässler, T. F. *Inorg. Chem.* **1990**, *29*, 4594.
(23) Burdett, J. K.; Chung, J. T. *Inorg. Chem.* **1993**, *32*, 750.
(24) Burdett, J. K.; Mitchell, J. F. *Inorg. Chem.*, in press.

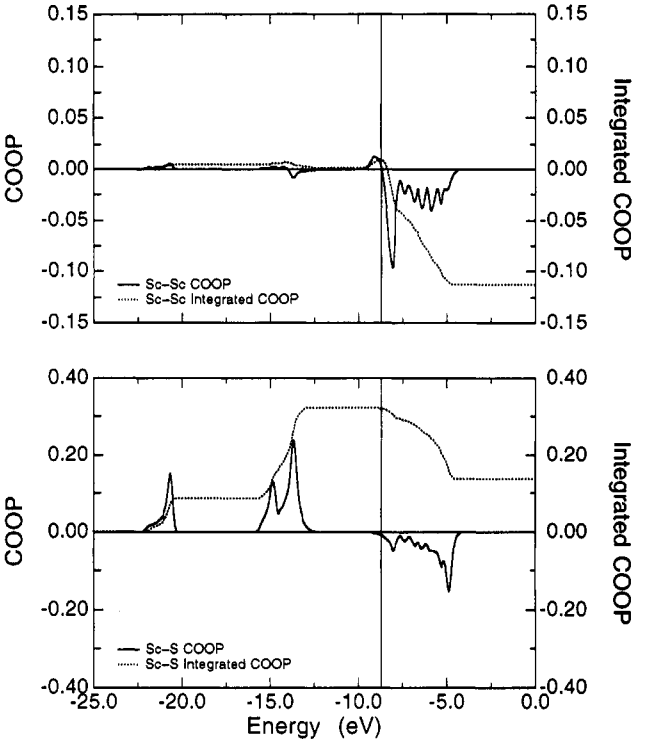


**Figure 2.** Crystal orbital overlap population (COOP) plots for stoichiometric ScS using charge-iterated parameters. Vertical line denotes the Fermi level for a $d^1$ transition metal.

pairs for the $d^1$ electron count. If such were the case, we could envision the metal nonstoichiometry in the $Sc_{1-x}S$ system as arising from an instability of the 1:1 compound, an idea akin to the rigid-band arguments of Denker,[25] with the difference that we are concerned with Sc–Sc interactions, not Sc–S interactions. It is important to note that calculation of the Sc–Sc pair potential includes "through-bond" interactions mediated by S, with similar considerations appropriate for the S–S pair potential. The details of the computation of such pair potentials are described elsewhere.[19] Briefly, a positive pair potential, $\Phi$, indicates a repulsive interaction. Small values of $\Phi$ manifest themselves as distortions away from the reference structure, but for large $\Phi$, the atom may be expelled from the structure.

The computed Sc–Sc pair potential is plotted as a function of electron count in the top panel of Figure 3. Interestingly, it is close to zero throughout the range of electron counts of interest, probably due to the large distance between the metal atoms. The bottom panel of Figure 3 shows the computed S–S pair potential in ScS along with the O–O pair potential for TiO in a hypothetical rocksalt structure. (The observed structure of TiO contains both metal and oxygen vacancies.) Clearly these two systems behave very differently. First, the S–S pair potential is essentially zero throughout $d^0$ to $d^3$, a desirable result in light of the fact that the S sublattice in $Sc_{1-x}S$ remains intact. Perhaps more interesting is the O–O pair potential. With a formal $d^2$ electron count TiO lies in a region of strongly repulsive O–O pair potential, and we expect that O should leave the lattice. Indeed, TiO is a nonstoichiometric material with roughly 17% vacancies on each sublattice. We note an earlier conclusion[26] that oxygen atom loss in TiO and NbO is driven by metal–

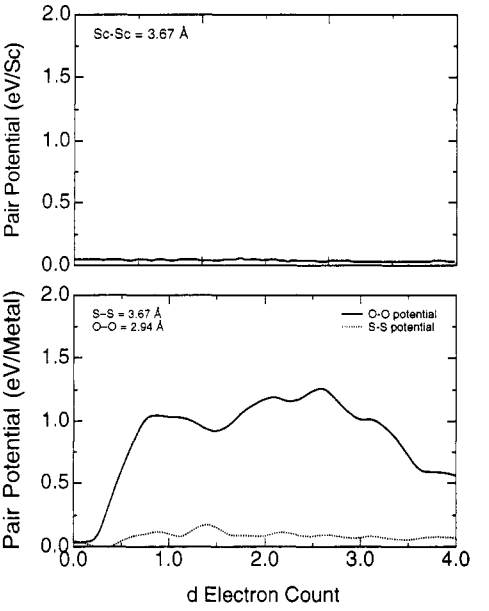


**Figure 3.** Pair potentials in rocksalt ScS. Bond length is taken from experiment. No iteration of extended Hückel parameters was performed. Top: Sc–Sc pair potential. Bottom: S–S and TiO O–O pair potentials.

metal bonding and some more recent discussion concerning pair potentials in these oxides.[24] The difference between the two plots in the bottom panel of Figure 3 may be interpreted in terms of the absence of generation of strong metal–metal interactions as anions are ejected from rocksalt ScS. The mechanism for the nonstoichiometry must be very different in the two systems.

Note that the O–O pair potential begins to have significant amplitude just above $d^{0.25}$. We also know from experiment that the alkaline earth oxides (e.g., MgO) are stoichiometric. The form of the O–O curve leads us to ask whether doping MgO or CaO with a transition-metal might produce a sudden onset of nonstoichiometry above this electron count. To date, there are numerous thermodynamic measurements of such solid solutions,[27,28] but no careful structural studies to test such an hypothesis.

To conclude this long discussion, it is clear that from the rigid-band viewpoint the loss of Sc gains nothing from the standpoint of either Sc–S or Sc–Sc bonding in ScS. We must therefore look beyond the rigid-band model to find a driving force for Sc vacancy formation. Before tackling this challenge, we first discuss the factors behind the adoption of the observed ordered defect structure of $Sc_{1-x}S$.

## Ordering in $Sc_{1-x}S$: A Cluster Model

The rocksalt structure is a cubic close-packed arrangement with both Sc and S in octahedral coordination. Structural studies of the $Sc_{1-x}S$ series show that as Sc leaves the lattice, the S atoms remain essentially fixed at the positions found for the $x = 0$ compound, despite the fact that the average coordination number monotonically decreases with $x$. The rigid-band model used above suggests that removing electrons from the Sc $t_{2g}$ band will have little or no effect on the bonding in ScS. This is clearly a simplification. Certainly the reduced coordination about Sc will show up in the S 3p bands in some way,

(25) Denker, S. P. *J. Less-Common Met.* **1968**, *14*, 1.
(26) Burdett, J. K.; Hughbanks, T. *J. Am. Chem. Soc.* **1984**, *106*, 3101.
(27) Davies, P. K.; Navrotsky, A. *J. Solid State Chem.* **1983**, *46*, 1.
(28) Davies, P. K.; Navrotsky, A. *J. Solid State Chem.* **1981**, *38*, 264.

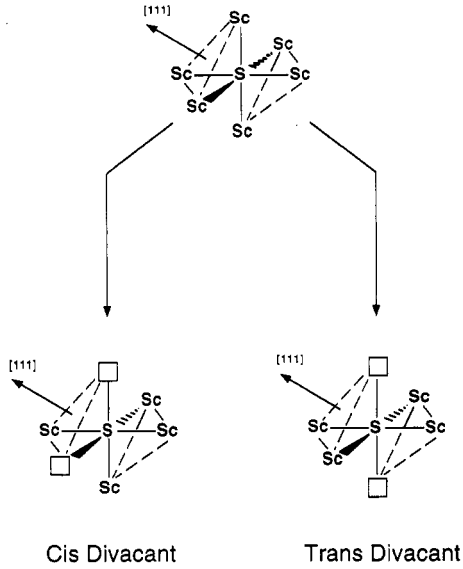


**Figure 4.** Effect of local geometry around sulfur as Sc vacancies are introduced.

and later we will comment on such effects in relation to the driving force for nonstoichiometry. Here we consider a simple cluster model to understand the observed ordering pattern of Sc vacancies in alternating (111) planes.

The top of Figure 4 shows a $SSc_6$ octahedron, the local geometry at a S site in the stoichiometric phase. The [111] direction is indicated, and the (111) metal planes perpendicular to it are suggested by the triangles of Sc atoms forming opposite faces of the octahedron. As Sc vacancies are formed, a certain fraction of the S atoms will have a single vacancy, some will have two vacancies, etc. The first structure for which there is some flexibility is the divacant structure, which may exist in two forms, *cis* and *trans*. As Figure shows, the *cis*-divacant structure has all vacancies in a single (111) plane, while the *trans*-divacant (square planar) structure has vacancies in both. In this sense, the cis structure is a model for the ordered $Sc_{1-x}S$ while the trans structure is a model for the disordered phase. Indeed, considering the extended structure, in the ordered phase there are *no trans*-divacant octahedra about S. We now provide arguments based on angular overlap and extended Hückel calculations that show an energetic preference for the *cis*-divacant structure, hence providing a rationale for the observed ordering pattern in the $Sc_{1-x}S$ series.

The energies from the angular overlap model (AOM)[29,30] for the $SSc_6$ unit, where the central S atom has only p orbitals (recall the DOS in Figure 1 and the relative unimportance of S 3s) and the Sc atoms only d orbitals, is shown in Figure 5. As expected from symmetry arguments, the octahedron has a trio of degenerate $t_{1u}$ levels, while the trans and cis structures have "two-below-one" and "one-below-two" patterns, respectively. Note that the square planar trans structure has its singleton at very high energy. The parameters $e_\sigma$, $e_\pi$, $f_\sigma$, and $f_\pi$ are just the second- and forth-order terms of the AOM. The energy differences between the two local structures as a function of electron count are given in Figure 5. Note that the plot starts at two electrons (filled S 3s orbital). For most electron counts the trans structure is energetically favored,

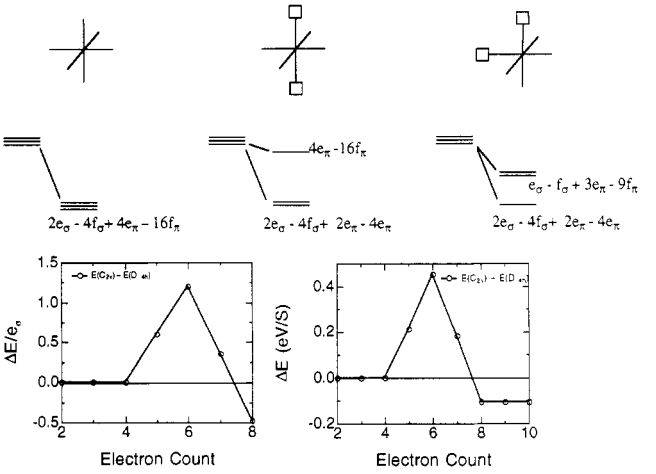


**Figure 5.** MO diagrams for various S-centered geometries. The 3s orbital on S is assumed filled. The graphs at the bottom show the energy differences for square planar vs octahedron and butterfly vs octahedron for AOM (left) and extended Hückel (right). In the AOM plot, $e_\sigma:e_\pi:f_\sigma:f_\pi$ = 1:0.2:0.1:0.02.

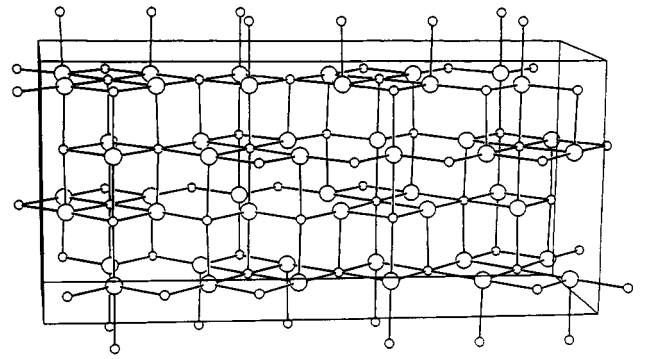

**Figure 6.** ORTEP drawing of the $Sc_2S_3$ structure. Small circles: Sc. Large Circles: S.

but at eight electrons the cis structure is more stable. Similar results are found from calculations at the extended Hückel level: the cis structure is favored by roughly 0.1 eV at $d^0$ and above. In these more complete calculations it is important to note that throughout the nonbonding levels (8–10 electrons), the energy difference is constant, indicating that metal–metal bonding plays a rather negligible role in the ordering process. Thus, the $Sc_{1-x}S$ structure orders its vacancies to relieve the energetic penalty paid by forming square planar S atoms, a coordination geometry which might be found in the disordered phase when entropic effects can populate unfavorable geometries. It is worthwhile noting that to our knowledge S is not found in square planar coordination in the crystal structure of any inorganic solid. Even more compelling, the structure of $Sc_2S_3$—shown in Figure 6—has all S atoms divacant in a cis arrangement.[10,31] Interestingly, $Sc_2S_3$ possesss a spiral arrangement of vacancies and is structurally quite different from the $Sc_{1-x}S$ family. Nevertheless, the *cis*-divacant S atoms in this $d^0$ compound argue for the importance of this coordination geometry.

## Ordering in $Sc_{1-x}S$: Extended Structure Models

The cluster models described above lead to a useful proposal for the preferential ordering of vacancies into alternating (111) planes. To model the extended lattice

(29) Burdett, J. K. *Adv. Inorg. Chem. Radiochem.* **1978**, *21*, 113.
(30) Burdett, J. K. *Molecular Shapes*; Wiley: New York, 1980; p 142.
(31) Kim, S.-J.; Anderegg, J. W.; Franzen, H. F. *J. Less-Common Met.* **1990**, *157*, 133.

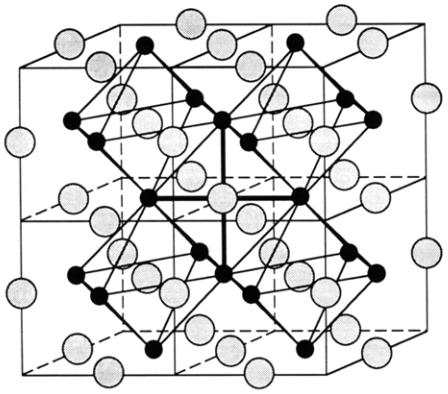

**Figure 7.** Four unit cells of hypothetical $Sc_3S_4$ emphasizing local coordination arount the two inequivalent S sites. Small circles: Sc. Large circles: S.

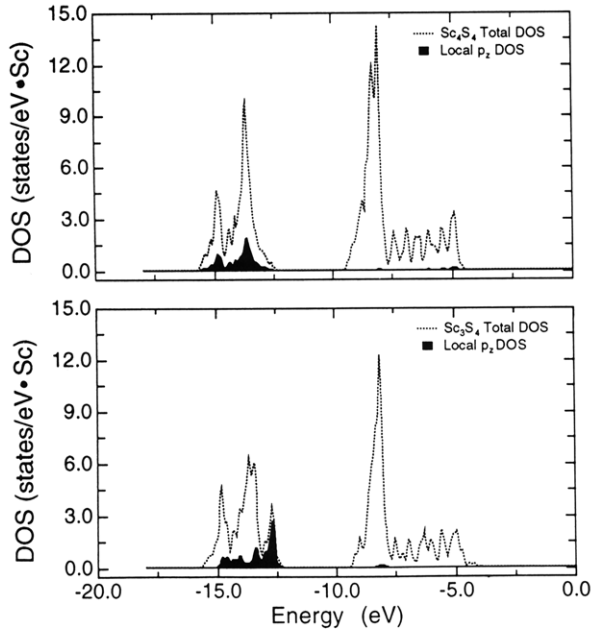


**Figure 8.** Effect of square planar S coordination on DOS of $Sc_{1-x}S$.

we turn to band structure calculations on model structures, noting that there is no simple way to accurately model these $Sc_{1-x}S$ phases. Even the low temperature "ordered" phase is disordered in the partially occupied (111) planes, so that there is no unit cell with a translational repeat. However, reasonable supercells of rocksalt that approximate the disordered and ordered phases may be chosen. The results show strong similarities to those from the cluster models, justifying the local model of the ordering process.

We first examine a hypothetical structure of stoichiometry $Sc_{0.75}S$, or $Sc_3S_4$. Figure 7 shows the supercell chosen, emphasizing the two different coordination geometries about S, octahedral, and square planar. We note that this cell is the same as that chosen by Misemer et al.[13] in their study of the defect scandium sulfides. These authors did not comment on the fact that the ordered phase cannot have *trans*-divacant S atoms and did not suggest a mechanism for vacancy formation or ordering. Our extended Hückel calculations give the band structure shown in the bottom panel of Figure 8. Here the total DOS and a projection of the S 3p orbitals orthogonal to the square planes are superimposed. Comparison of this DOS to that of the stoichiometric analog (upper panel)

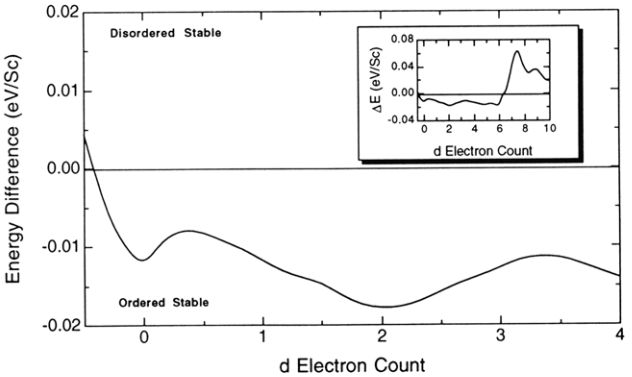


**Figure 9.** Energy difference curve between the supercell models of the ordered and disordered phases of $Sc_{0.78}S$ in the early $t_{2g}$ band filling region. Inset: Expansion of curve showing full d band region.

shows that very little is happening in the $t_{2g}$ band, but that a distinct peak arises in the S 3p band. This peak was noted by Misemer and is clearly due to the presence of the square planar S atoms, a feature noted above for the cluster calculations. Clearly, this model is not suitable for studying the ordering, as there is no corresponding supercell with the appropriate vacancy distribution. It is useful, however, for showing that S in the solid "remembers" its local coordination environment.

The observed stoichiometry in the congruently vaporizing phase of $Sc_{1-x}S$ is $Sc_{0.8065}S$.[32] We have generated two supercells with stoichiometry $Sc_{0.78}S$, a close approximation. These supercells were formed by putting vacancies into the (0001) planes of a hexagonal cell of rocksalt; equally distributed in the "$[1-x,1-x]$" structure and alternating with fully occupied layers in the "$[1,1-2x]$" structure. On the basis of Figure 4 from the cluster models, we predict a mixture of *cis*- and *trans*-divacant octahedra in the $[1-x,1-x]$ phase and only *cis*-divacant octahedra in the $[1,1-2x]$ structure.

Figure 9 shows the energy difference curve between model supercell structures as a function of electron count. Note in the inset a discontinuity at $d^6$, a signature of an "$e_g$ effect." The main part of the Figure focuses on the crucial $t_{2g}$ region of band filling and shows a small energy preference for the ordered supercell throughout these electron counts. Importantly, the structural preference changes over from disordered to ordered just before $d^0$ and does not vary considerably in the region of interest, a favorable parallel to the cluster calculations of Figure 5. Although the energy differences here are small, the similarities between the cluster calculations and the supercell models indeed suggest tha the dominant effects are coming from the S 3p bands. Particularly that the driving force for ordering is associated with the loss of square planar S atoms, as asserted in the cluster calculations.

## Ordering: The Method of Moments

We would like to complement this "classical" description of the electronic driving force for ordering with a less conventional approach based on the method of moments.[33-35] We build here on the discussions of our recently

(32) Tuenge, R. T.; Laabs, F.; Franzen, H. F. *J. Chem. Phys.* **1976**, *65*, 2400.

(33) Burdett, J. K.; Lee, S.; Sha, W. C. *Croat. Chim. Acta* **1984**, *57*, 1193.

developed electronic model for order–disorder transitions,[15] where the foundation was laid for applying the method of moments to disordered systems in a mean-field sense. Whereas that discussion was purely abstract in nature, we are interested here in applying those ideas to a concrete example, the vacancy ordering of $Sc_{1-x}S$. As in the models from our recent work on order–disorder transitions,[15] we are considering an ABAB ordering pattern, but here A and B represent a partially occupied layer and a stoichiometric layer, respectively. As the system cools, we are interested in the preference of the ordered pattern over the disordered pattern—a fourth moment problem.

On the basis of arguments similar to those of Burdett and Kulkarni in a study of defect perovskites,[36] we expect the idealized energy difference curve as a function of fractional band filing, $x$, to have the form shown in 2,

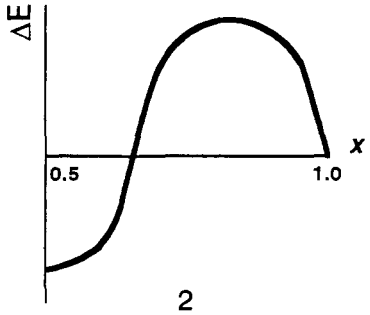


2

where the system with the smaller fourth moment is stable in the region surrounding the half-filled point. For the ScS solid, since the S levels are Sc–S bonding and the Sc d levels Sc–S antibonding, the half-filled point lies at $d^0$. Our results from ref 15 showed that with a half-filled band the ABAB pattern is favored. With ~0.5 d electrons, $Sc_{0.8065}S$ certainly lies near the half-filled $d^0$ point, and its observed ordering pattern agrees with the predictions from the moments theory for the linear chain. Let us now explore the extension of these ideas to the $Sc_{1-x}S$ system to see if they indeed hold true.

Despite the three-dimensional nature of the rocksalt structure, the vacancy ordering in $Sc_{1-x}S$ is along one direction only, simplifying matters to a quasi-one-dimensional problem. We consider three parameters, $\alpha_{Sc}$, $\alpha_S$, and $\beta$, representing the on-site energy of Sc, that of S, and the transfer (or hopping) integral between them. The probabilities of occupation in any two adjacent layers will be designated $P_1$ and $P_2$, with the constraint that $P_1 + P_2 = 2(1 - x)$, where $1 - x$ is obviously the average fractional occupancy factor. The simplest approximation is then to write a linear function with an order parameter $y$ which takes values from 0 (disordered) to $x$ (ordered). Of course, for all nonzero $x$ this order parameter can be normalized to the interval [0,1] by dividing through by $x$:

$$P_1 = 1 - x + y$$

$$P_2 = 1 - x - y \qquad (1)$$

Following the procedure of ref 15, we form the four basis pattern probabilities enumerated in Table I. Each of these probabilities is based on the [1,1 – 2$x$] low-temperature ordering pattern and gives rise to a one-dimensional supercell with two layers. Naturally, when all four possibilities are tabulated, the summed probability must be unity. Each of these basis patterns corresponds to a specific structure, whose Hückel hamiltonian can be enumerated readily. We then form the probability-weighted linear combination of the four basis patterns and evaluate the moments. We define the difference in the $i$th moment by $\Delta\mu^i(\bar{y}) = \mu^i(x,\bar{y}) - \mu_i(x,\bar{y}=0)$, where $\bar{y}$ is the renormalized order parameter. As expected, the first nonzero $\Delta\mu^i(\bar{y})$ is the fourth, and its value is (per Sc site)

$$\Delta\mu^4(\bar{y}) = -60\beta^4x^2\bar{y}^2 \qquad (2)$$

The minimum value of this function occurs at $\bar{y} = 1$, or $y = x$. That is, the fourth moment difference is minimized at the [1,1 – 2$x$] pattern, the observed ordering at half-filling.

Using a strictly one-dimensional analog, we can explain these results in terms of available walks from S. 3 shows

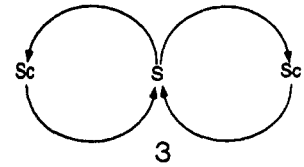


3

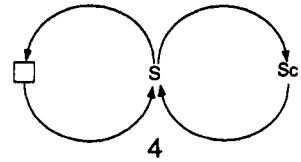


4

the crucial walk of length four originating and terminating on a given S site. The Sc atoms on either side represent different metal planes, of course. The probability functions $P_1$ and $P_2$ given in eq 2, when multiplied together, give the joint probability of finding two adjacent Sc planes occupied. In Figure 10 we plot this joint probability as a function of $x$ for several values of $\bar{y}$. The plots clearly show that, independent of $x$, the maximum value of the probability comes at $\bar{y} = 0$, and the minimum at $\bar{y} = 1$. Thus, for the $\bar{y} = 0$ case we have the greatest probability of finding walks of the kind in 3, whereas in the $\bar{y} = 1$ case, we are guaranteed that these walks are absent, as shown in 4. This immediately shows that the fourth moment must be maximized for the disordered phase (where the walks are available), and minimized in the ordered phase

**Table I. Basis Pattern Probabilities for $Sc_{1-x}S$**

| layers occupied | probability[a] |
|---|---|
| 1, 2, 3, 4, 5, 6 | $P_1 \cdot P_2 = (1-x)^2 - y^2$ |
| 1, 3, 5 | $P_1 \cdot (1-P_2) = (x+y)(1-x+y)$ |
| 2, 4, 6 | $(1-P_1) \cdot P_2 = (x-y)(1-x-y)$ |
| none | $(1-P_1) \cdot (1-P_2) = x^2 - y^2$ |

[a] Summed probabilities = 1.

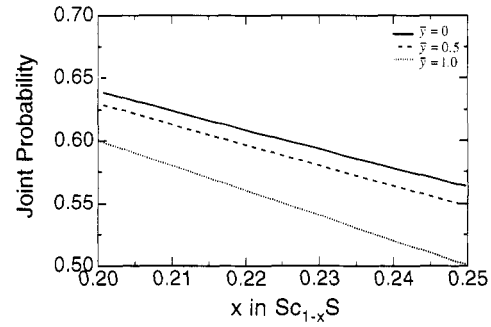


**Figure 10.** Joint probability of finding Sc atoms on adjacent (111) planes as a function of stoichiometry ($x$) and order parameter ($\bar{y}$).

(34) Burdett, J. K.; Lee, S. *J. Am. Chem. Soc.* **1985**, *107*, 3063.
(35) Burdett, J. K.; Lee, S. *J. Am. Chem. Soc.* **1985**, *107*, 3050.
(36) Burdett, J. K.; Kulkarni, G. V. *J. Am. Chem. Soc.* **1988**, *110*, 5361.

(where the walks are missing). At the half-filled point the structure with the smaller fourth moment is stable, in agreement with the observation of the $[1,1-2x]$ ordering in the $Sc_{1-x}S$ system.

### Sc Vacancy Formation in ScS

We now turn our attention to the other challenge presented by $Sc_{1-x}S$, namely, why Sc vacancy formation is energetically favored. As a reviewer pointed out, our chemical intuition suggests that $Sc^{2+}$ should be unstable with respect to $Sc^{3+}$; that is, the +3 oxidation state of Sc is generally considered "more stable" than the +2 state, and vacancy formation should increase the proportion of formally +3 Sc atoms. Defining what is meant by the stability of one oxidation state over another in the solid state is a compelling theoretical challenge which rests in the competition between localized and extended electronic states. Clearly, the balance between the cost of ionizing an electron and the gain from bond formation is a key component, but other factors are certainly at work as evidenced by the oxide superconductors. Understanding such factors will require calculations more sophisticated than our one-electron models. For $Sc_{1-x}S$, as shown by conductivity measurements,[10] the third Sc electron is best considered as lying in a delocalized state, so that we may *formally* assign a +3 charge to all Sc atoms, satisfying our chemical intuition. Nonetheless, the third electron, while delocalized, clearly lies in a band of essentially all Sc character, so that removal of this electron must effectively oxidze the Sc atoms to some extent, though not from $Sc^{2+}$ to $Sc^{3+}$. For the present, we are forced to seek another explanation for vacancy formation. Our approach to understanding Sc vacancy formation is to go beyond a simple rigid-band model in investigating the effect of vacancies on the electronic structure of ScS. We begin with the parent material.

### Effect of Vacancy Formation on the Band Structure

The rocksalt structure is a stable structure adopted by the alkaline-earth sulfides, which are stoichiometric, and so it is the availability of a manifold of d states in the transition metals which is in some way responsible for the generation of nonstoichiometry. An early explanation for the vacancy formation in the rocksalt systems was provided by Denker,[25] who argued from cluster analogs and rigid-band considerations that depletion of electrons from the d bands would relieve antibonding metal–anion interactions. Although appealing, this explanation is lacking in view of Figure 1 which shows the $d^1$ fermi level for stoichiometric ScS lying below the onset of the antibonding states. We have also seen that metal–metal bonding, though weak, would be sacrificed upon oxidation. Furthermore, rigid-band arguments necessarily require loss of one-electron energy as the band is depleted of electrons. Huisman et al. recognized this fact in their study of vacancy formation in TiO and TiC.[37] These researchers suggested four factors responsible for vacancy stabilization: (1) band mean energy changes, (2) bandwidth changes, (3) appearance of new defect bands, and (4) Fermi level position. They based their results on a two-band model which

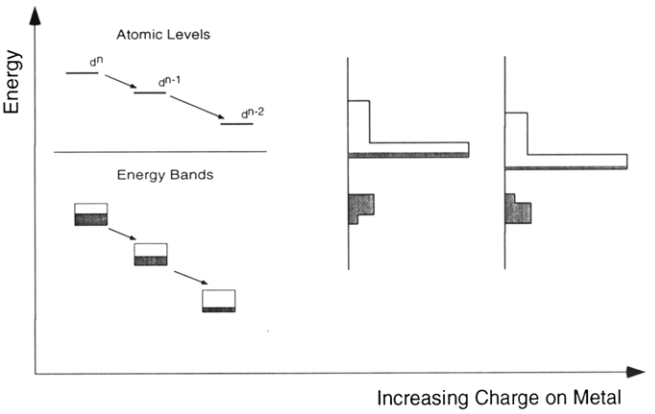


**Figure 11.** Effect of oxidation on energy levels in molecules and extended solids. Left: first-order variation of band energy with charge. Right: second-order effect of increased mixing of d character into anion p band.

involved placing an artificial vacancy band at an electronegativity above the metal band but not at infinite energy. They maintained that the occupancy of these defect states with electrons from the Ti bands stabilizes the system. Our model does not introduce any such levels explicitly but takes care of the different coordination environments using a supercell approach. Our model of vacancy formation combines parts (1) and (4) of Huisman's approach, but another vital factor is introduced which is responsible for vacancy stabilization in the early transition metal sulfides.

There are two major effects on the band structure as Sc atoms are removed. Since there is a large electronegativity difference between Sc and S, the loss of a Sc atom with its three electrons leads to oxidation of the remaining Sc atoms. Such oxidation implies that the remaining Sc atoms become more electronegative. The first-order response of the band structure will thus be to lower the energy of the Sc levels, and in particular the Sc d band. Such a process is indicated schematically on the left of Figure 11, along with the cluster analogy. We note that such an effect will be most potent when the electrons are depleted from orbitals that are largely—or exclusively—metal located. If the electrons of the parent $Sc_{1.0}S$ were in orbitals of mixed metal and anion character, this effect would be significantly attenuated. We will return to this point later. This lowering of the d levels leads to a change in the magnitude of metal-d/anion-p interaction. We know from second-order perturbation theory that this mixing of orbitals is controlled by their energy separation.[38] Hence, as the d band drops in energy, we should expect to see a larger interaction between the Sc 3d and S 3p orbitals, with an extra stabilization of the latter. Of course, the d orbitals involved in this mixing lie above the $t_{2g}$ states and are empty, the equivalent of a "two orbital–two electron" stabilization from molecular orbital theory. The right-hand panel of Figure 11 sketches the elements of this mechanism, indicating the shift in the S 3p DOS to lower energies upon mixing. We now have a model for stabilizing vacancies in the *early* transition-metal sulfides adopting the rocksalt structure. These systems have few d electrons which are located at the bottom of the $t_{2g}$ band, a region of the DOS that is exclusively metal character and hence most likely to exhibit strong stabilization upon

(37) Huisman, L. M.; Carlsson, A. E.; Gelatt, C. D., Jr.; Ehrenreich, H. *Phys. Rev. B: Solid State Phys.* **1980**, *22*, 991.

(38) Albright, T. A.; Burdett, J. K.; Whangbo, M.-H. *Orbital Interactions in Chemistry*; Wiley: New York, 1985.

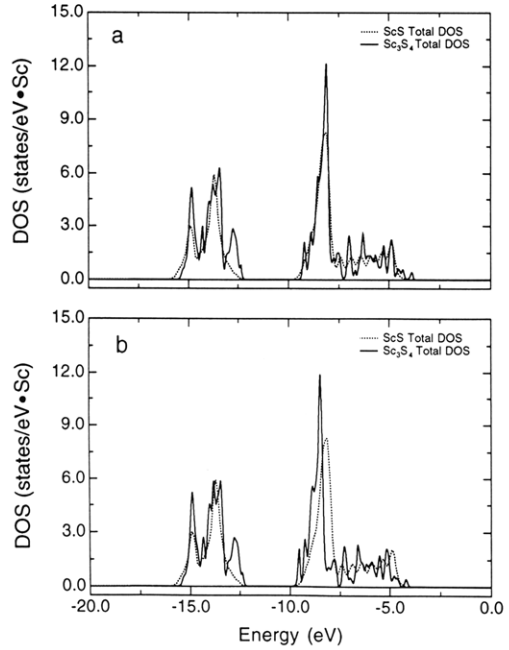


**Figure 12.** DOS for $Sc_3S_4$ and ScS (a) without and (b) with charge-iteration.

oxidation. As the d band edge drops in these materials, the energy gap between it and the S p band closes, reinforcing the second-order mixing in this anion band and thereby stabilizing the defect structure.

This hypothesis may be tested by studying the effect(s) of increasing $x$ on the extended Hückel band structure. Such calculations are accomplished by charge-iterating the energies of Sc orbitals ($H_{ii}$) as a function of their electron occupation.[39,40] In eq 3 $H_{ii}$ is written as a quadratic function of the charge, $q$, where the parameters $A$, $B$, and $C$ are obtained from atomic spectral data.[41] (Our parameters are tabulated in the Appendix.)

$$H_{ii}(q) = A + Bq + Cq^2 \qquad (3)$$

First, we consider the $Sc_3S_4$ structure encountered earlier in Figure 7. There we saw that the predominant effect on the DOS on introducing vacancies was the splitting off of a p orbital from the S band; the Sc d band being little changed. Figure 12 shows that the effects described above are indeed pronounced. In the top panel, the DOS of stoichiometric ScS is superimposed on that of $Sc_3S_4$ without iteration. Despite the peak structure on the $Sc_3S_4$ DOS, the d bands of these systems are indeed very similar. Turning on charge-iteration yields the results in the bottom panel. Note first that in the S 3p region there is a small stabilization of the DOS of $Sc_3S_4$ relative to that of ScS when charge iteration is included. However, the Sc $t_{2g}$ band has shifted significantly to lower energies as a result of vacancy formation, in accord with the discussion above. To further emphasize this point, we plot in Figure 13 the variation of Fermi level with electron count for $Sc_3S_4$ with and without iteration. The main part of the figure shows that the Fermi level for these calculations is essentially the same until the d band begins to fill above $d^0$ (32 electrons), at which point the Fermi level of the iterated system drops. The inset shows that this difference is a substantial 0.4 eV. Additionally, the inset shows that the difference is constant above ~35 electrons ($d^1$). Thus, the effects of increased charge are felt only at extremely low electron counts.

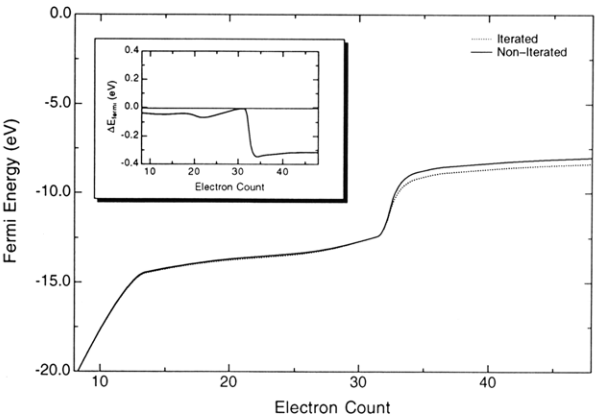


**Figure 13.** Comparison of Fermi levels of iterated and noniterated $Sc_3S_4$ as a function of electron count. Inset: difference between the two curves in the main figure. Note that $d^0$ is at 32 electrons, $d^{0.33}$ at 33 electrons, and $d^1$ and 35 electrons.

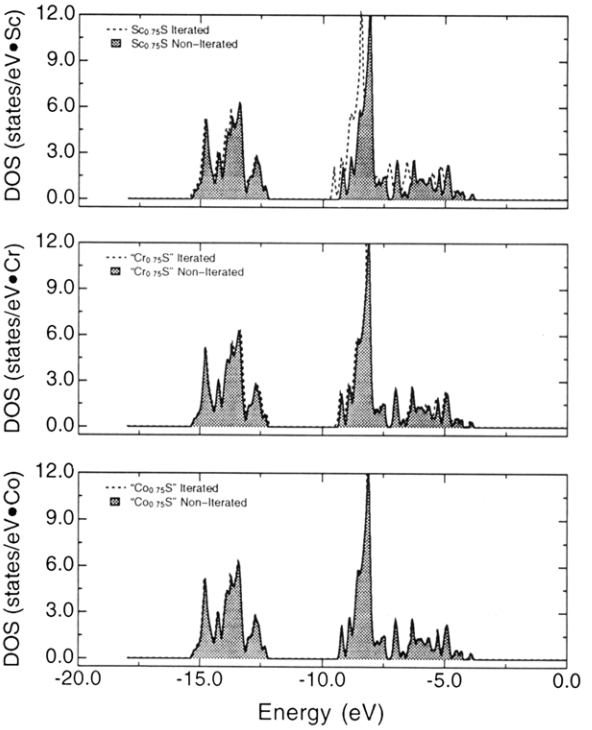


**Figure 14.** Total DOS of iterated and noniterated $Sc_{0.75}S$, "$Cr_{0.75}S$" and "$Co_{0.75}S$."

We can get a better sense of the effect of band filling on the iteration by putting more electrons into the system. Calculations at higher electron counts dramatically show the diminished effect of iteration as the d band fills above the metal-located levels. The series of calculations whose results are shown in Figure 14 were carried out using the $Sc_{0.75}S$ coordinates and parameters; only the number of electrons was increased to produce the hypothetical "$Cr_{0.75}S$" and "$Co_{0.75}S$" (the binary sulfides of Cr and Co do not form rocksalt phases). Note that from $Sc_{0.75}S$ to "$Cr_{0.75}S$" to "$Co_{0.75}S$" the iterated DOS becomes progressively more like the noniterated DOS. In particular, that the "$Co_{0.75}$" is essentially indistinguishable from that of

(39) Basch, H.; Viste, A.; Gray, H. B. *Theor. Chim. Acta* **1965**, *3*, 458.
(40) McGlynn, S. P.; Vanquickenborne, G.; Konoshita, M.; Carroll, D. G. *Introduction to Applied Quantum Chemistry*; Holt, Rheinhard and Winston: New York, 1972.
(41) Moore, C. E. *Ionization Potentials and Ionization Limits Derived from the Analyses of Optical Spectra*; National Bureau of Standards: Washington, D.C., 1970.

**Table II. Extended Hückel Parameters for Transition-Metal Oxides and Sulfides**

| | atom | | $H_{ii}$ (eV) d | $H_{ii}$ (eV) s | $H_{ii}$ (eV) p | orbital exponent d[a] | orbital exponent s | orbital exponent p |
|---|---|---|---|---|---|---|---|---|
| standard | Sc | | -8.510 | -8.870 | -2.750 | 4.35 (0.427 78)<br>1.70 (0.727 57) | 1.300 | 1.300 |
| | Ti | | -10.810 | -8.970 | -5.440 | 4.55 (0.420 60)<br>1.40 (0.783 91) | 1.075 | 0.675 |
| | O | | | -32.300 | -14.800 | | 2.275 | 2.275 |
| | S | | | -20.000 | -13.300 | | 2.122 | 1.827 |
| iterated[b] | Sc | (ScS) | -8.289 | -7.370 | -4.288 | 4.35 (0.427 78)<br>1.70 (0.727 57) | 1.300 | 1.300 |
| | Ti | (TiO) | -11.434 | -9.364 | -5.719 | 4.55 (0.420 60)<br>1.40 (0.783 91) | 1.075 | 0.675 |

[a] Double-$\zeta$ expansion of metal d orbitals. Coefficients of each function are given in parentheses. [b] System iterated is given in parentheses after corresponding metal.

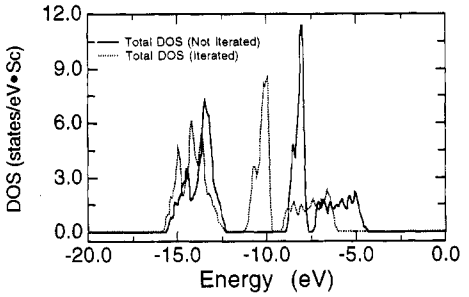


**Figure 15.** DOS of $Sc_2S_3$ comparing results from noniterated and iterated parameters.

"$Sc_{0.75}S$." Of course, this is precisely the result suggested qualitatively above. Only low d count systems, where there is occupancy of levels which are virtually all metal in character, will show such shifts on oxidation. The admixture of S character into the metal d orbitals at higher energies very effectively dilutes the effect of the charge on the metal, reducing the shift in $H_{ii}$ to lower energies. Hence, only low d count systems will be susceptible to promotion of metal vacacny formation via d band stabilization.

We noted above that the second-order effect of the band shift is to stabilize the anion bands. Crucial to this is a smaller separation between these levels and the d band. One measure of such a separation is the calculated bandgap between the top of the anion valence band and the metal conduction band. We note that this is not necessarily a direct measure of the separation between the pertinent anion levels and the d band, as the top of the valence band is predominantly nonbonding between Sc and S. Nonetheless, the band gap is a semiquantitative measure of the energy separation and hence the strength of interaction between Sc d and S p bands. Figure 15 shows a comparison of the density of states of $Sc_2S_3$ with and without charge iteration. Note the strong downward movement of the Sc $t_{2g}$ band, and, equally significant, the fact that the peaks in the S p band have shifted to lower energies, in complete accord with the expectations of the model. Note also that this interaction is significantly more potent than that in the $Sc_3S_4$ calculations (Figure 14). Recalling that $Sc_2S_3$ has no *trans*-divacant S atoms, such a result further evinces the electronic stabilization of removing square planar S sites from $Sc_{1-x}S$. These calculations suggest that our novel electronic mechanism is indeed a viable route for stabilizing metal vacancies in these early transition metal systems. Of course, detailed numerical considerations of systems with different stoichiometry are inappropriate using our one-electron model.

**Table III. Charge-Iteration Parameters**

| Sc/Ti metal | *A* | *B* | *C* |
|---|---|---|---|
| 3d | 2.287 | 9.583 | 6.200 |
| 4s | 1.200 | 6.250 | 6.020 |
| 4p | 0.970 | 4.410 | 3.330 |

## $Sc_{1-x}S$: Summary of Theoretical Results

Using cluster models and extended Hückel calculations on large supercells, we have demonstrated that metal–metal bonding plays an insignificant role in the ordering process of vacancies in $Sc_{1-x}S$. Rather, it is the transformation of square planar S atoms to *cis*-divacant "butterflies" that drives the ordering of Sc vacancies into alternating (111) planes. Corroborating these results were ideas from the method of moments, which indicated that the fourth moment was minimized in the ordered structure, energetically favored for the half-filled band. We view metal vacancy formation as arising from a combination of first-order shifts in the Sc d band with increasing nonstoichiometry, and second-order mixing of the Sc 3d and S 3p bands. These effects are intimately connected, as it is the lowering of the d band that enhances the second order mixing. Charge-iteration calculations on a series of $Sc_{1-x}S$ model systems showed qualitatively the validity of such a model. Perhaps most importantly, we showed that this mechanism is only operative for systems with a few d electrons, as systems with higher Fermi levels lose the first-order stabilization of the d band. Indeed, it is precisely for the early transition-metal sulfides that this kind of nonstoichiometry is observed. As pointed out at the beginning of this paper, $Sc_{1-x}S$ appears from experimental data to be a prototype for most of the group 3 and 4 transition-metal sulfides, leading us to believe that our work here provides at least a qualitative framework for understanding the vacancy formation and ordering throughout this entire series of binary sulfides.

**Acknowledgment.** This work was conducted under NSF DMR 8819060. J.F.M. acknowledges the generous support of the Fannie and John Hertz Foundation.

## Appendix

All calculations were of the extended Hückel tight-binding type. Parameters are tabulated in Table II. For charge-iteration calculations, the pertinent parameters are tabulated in Table III.